Collective bands in doubly-even Sn nuclei: Energy spectra and electromagnetic decay properties

G. Wenes, P. Van Isacker, and M. Waroquier
Institute of Nuclear Physics, Proeftuinstraat 86, B-9000 Gent, Belgium

K. Heyde and J. Van Maldeghem
Institute of Nuclear Physics, Proeftuinstraat 86, B-9000 Gent, Belgium
and Institut de Physique Nucléaire (and IN2P3), Université Lyon-1,43 Bd du 11 Novembre 1918, 69622 Villeurbanne-Cedex, France
(Received 18 November 1980)

Starting from a simplified description, treating proton two-particle two-hole (2p-2h) excitations coupled with spherical quadrupole vibrations in interaction with the low-lying quadrupole vibrational states in doubly-even $^{112-118}$Sn nuclei, we are able to account for the regular $\Delta J = 2$ band structure on top of excited $J^\pi = 0^+$ states. Energy spectra as well as $E2$ and $E0$ decay properties are calculated and are extensively compared with recent experimental data.

[NUCLEAR STRUCTURE Proton 2p-2h–core coupling calculations, collective bands in $^{112-118}$Sn; energy spectra, $E2$ and $E0$ transitions.]

I. INTRODUCTION

The structure of doubly-even Sn nuclei is generally described in terms of neutron excitations, assuming an inert $Z=50, N=50$ core. In the BCS approach,[1,2] using neutron two-quasiparticle calculations, the experimental data can be described rather well.

Different modes of excitation can, however, be distinguished in the neighboring In (Ref 3–5) and Sb (Ref. 6–8) isotopes. In order to account for *all* low-lying levels in these odd-mass nuclei, one has to introduce proton particle-hole excitations through the $Z = 50$ closed proton core in order to account for the observed band structure, built on top of the $J^\pi = \frac{1}{2}^+$ and $\frac{9}{2}^+$ levels in In and Sb, respectively. Starting from a vibrational picture, the explicit treatment of 2h-1p (Ref. 5) and 2p-1h (Ref. 7) configurations, coupled to quadrupole vibrations of Sn nuclei, is necessary. Recently, experimental evidence for the observation of excited $J^\pi = 0^+$ states in doubly-even Sn (Refs. 9,10) and Cd (Ref. 11) nuclei became available. These levels are strongly excited via the (^{3}He,n) two-proton transfer,[12] thus suggesting the importance of proton two-particle two-hole (2p-2h) configurations.

Therefore, we have constructed a simplified model taking into account both pure quadrupole vibrational excitations of doubly-even nuclei as well as proton 2p-2h configurations coupled with quadrupole vibrational excitations. The nuclear Hamiltonian, the nuclear wave functions, the parameters used, and the approximations carried out are discussed in Sec. I. In Sec. II, the energy spectra for $^{112-118}$Sn are compared with experiment, and also electromagnetic $E2$ and $E0$ decay properties are extensively discussed in view of the recent experimental data.

II. PROTON TWO-PARTICLE TWO-HOLE (2p-2h) EXCITATIONS

A. Hamiltonian and wave functions

A general Hamiltonian, describing an interacting system of boson and fermion degrees of freedom, can be written as

$$H=\sum_{\lambda\mu} b^\dagger_{\lambda\mu} b_{\lambda\mu}(\hbar\omega_\lambda+\tfrac{1}{2})+\sum_\alpha \epsilon_\alpha c^\dagger_\alpha c_\alpha-\sum_{\substack{\alpha\beta\\ \lambda\mu}}\left(\frac{\pi}{2\lambda+1}\right)^{1/2}\xi_\lambda\hbar\omega_\lambda\sum_{\alpha\beta}\langle\alpha|Y_{\lambda\mu}|\beta\rangle[b^\dagger_{\lambda\mu}+(-1)^\mu b_{\lambda-\mu}]c^\dagger_\alpha c_\beta+\tfrac{1}{4}\sum_{\alpha\beta\gamma\delta} v_{\alpha\beta\gamma\delta}c^\dagger_\alpha c^\dagger_\beta c_\delta c_\gamma+V_{\text{Coulomb}} \tag{2.1}$$

where the first and second term describe the unperturbed energy of the boson and fermion systems, respectively. Here $\hbar\omega_\lambda$ denotes the λ-pole phonon energy and ϵ_a the single-particle(-hole) energy. The third term describes the interacting boson-fermion Hamiltonian with ξ_λ as the coupling strength (for its definition, see Refs. 13 and 14), whereas the fourth term describes the residual fermion interaction. Also, the Coulomb contribution for proton residual interactions is explicitly included.

Having in mind a possible description of collective bands in even-even Sn nuclei, resulting from the explicit interaction of proton 2p-2h excitations through the $Z = 50$ closed proton shell with the quadrupole vibrations of the underlying core nu-

cleus, the nuclear wave function can be expanded as

$$|i;JM\rangle = \sum c^i(NR;J)\,|NR;JM\rangle + \sum d^i((p_1p_2)J_p[(h_1h_2)J_h,NR]I;J) \times |(p_1p_2)J_p[(h_1h_2)J_h\otimes NR]I;JM\rangle , \tag{2.2}$$

where $N(R)$ denotes the number (angular momentum) of the quadrupole vibrational excitations (we only consider $\lambda=2$) and $p_1,p_2(h_1,h_2)$ the proton particle(-hole) configurations, respectively i.e., $1g_{7/2}$, $2d_{5/2}$, $2d_{3/2}$, $3s_{1/2}$, $1h_{11/2}$ and $1g_{9/2}{}^{-1}$, $2p_{3/2}{}^{-1}$, $2p_{1/2}{}^{-1}$, $1f_{5/2}{}^{-1}$. Whenever summation indices are not written below the summation symbol [see Eq. (2.2)], we imply summation over quantum numbers that occur in both the expansion coefficients (c^i,d^i) and the basis configurations $|\cdots\rangle$, except the total angular momentum, also appearing in the total wave function, at the left hand side of the equal sign. The expansion coefficients (c^i,d^i) are obtained by diagonalizing the nuclear Hamiltonian (2.1) within the basis discussed above. Already from Eq. (2.2), one observes that particular states in doubly-even Sn nuclei will be described mainly as pure quadrupole phonon excitations $|NR;JM\rangle$ ($d^i\simeq 0$), whereas other levels will mainly contain proton 2p-2h–core coupled configurations ($c^i\simeq 0$).

Instead of carrying out the full calculation immediately, we proceed in different steps, in order to obtain better insight in the final results.

(i) In a first step, only a particular part of the nuclear Hamiltonian is diagonalized (i.e., the Hamiltonian H', only containing the single-hole energy, the collective quadrupole vibrations of the Sn nuclei, the hole-core, and the hole-hole residual interactions) in order to obtain a description of the Cd eigenstates. Thereby, we solve the secular equation

$$H'\,|k;IM\rangle = \omega(I,k)\,|k;IM\rangle , \tag{2.3}$$

with

$$|k;IM\rangle = \sum a^k((h_1h_2)J_h,NR;I)\,|(h_1h_2)J_h\otimes NR;IM\rangle , \tag{2.4}$$

where $\omega(I,k)$ gives the energy spectrum (describing the Cd nuclei) and a^k gives the expansion coefficients. Such calculations have been carried out before in describing doubly-even Cd nuclei.[15-18] In these references, full details on the formalism can be found. In our calculations, the wave functions (2.4) only serve as an intermediate step to build more complicated configurations by subsequently coupling with proton 2p configurations. The lowest energy eigenvalue $\omega(0^+,1)$ describes the pairing gain in the proton 2h-Sn core system due to the pure 2h pairing as well as due to the residual 2h-core interaction. This energy value can also be obtained from known experimental proton separation energies[19] via the relation

$$\omega(0^+,1) = S_p(Z=50) - S_p\,(Z=49) . \tag{2.5}$$

(ii) In a second step, we couple the proton 2p configurations with the eigenfunctions (2.4) and obtain as a new basis the collective quadrupole vibrational configurations $|NR;JM\rangle$ and the proton 2p-Cd coupled configurations $|(p_1p_2)J_p\otimes Ik;JM\rangle$. The wave function (2.2) can therefore be transformed into the more transparent form

$$|i;JM\rangle = \sum c^i(NR;J)\,|NR;JM\rangle + \sum l^i((p_1p_2)J_p,Ik;J)\,|(p_1p_2)J_p\otimes Ik;JM\rangle . \tag{2.6}$$

This wave function is obtained by solving the secular equation corresponding with the full Hamiltonian (2.1) as

$$\begin{bmatrix} N_2\hbar\omega_2\delta_{NN'}\delta_{RR'} & L(NR;(p_1'p_2')J_p',I'k';J) \\ L((p_1p_2)J_p,Ik;N'R';J) & [\epsilon_{p_1}+\epsilon_{p_2}+\omega(I,k)]\delta_{\{O,O'\}} \\ & +K((p_1p_2)J_p,Ik;(p_1'p_2')J_p',I'k';J) \end{bmatrix} \tag{2.7}$$

where the L- and K-matrix elements are defined in Appendix A. Here, we also use the shorthand notation $\{O\}$ for all quantum numbers $\{p_1,p_2,J_p,I,k\}$. Since many (±200–300) proton 2p-Cd core-coupled configurations constitute the second part of the wave function (2.6), a still more transparent representation for describing the nuclear wave function can be obtained. Diagonalizing within the lower right part of the energy matrix (2.7) (defined as the $\mathfrak{K}$ matrix), containing only interactions within the proton 2p-Cd core configurations, bands with $\Delta J=2$ spin sequence are obtained. The particular wave functions are obtained as

$$|\mathrm{rot}(i);JM\rangle = \sum r^i((p_1p_2)J_p,Ik;J)\,|(p_1p_2)J_p\otimes Ik;JM\rangle , \tag{2.8}$$

for $i=1,2,\ldots N$, where N is the dimension of the 2p-Cd core configuration space and rot stands for rotational, due to the apparent similarities with collective, rotational energy spectra for the lowest bands (Fig. 1). One should, however, be

cautious in interpreting the label i for classifying energy eigenvalues, obtained from

$$\mathcal{H}|\,\mathrm{rot}(i);JM\rangle = E^i(\mathrm{rot};J)|\,\mathrm{rot}(i);JM\rangle\,. \qquad (2.9)$$

Only for the yrast sequence, i.e., $i=1$, does a one-to-one correspondence between the value i and the classification of eigenstates $|\,\mathrm{rot}(i);JM\rangle$ into a band exist. Here, a band is defined as a set of levels, strongly connected via the $E2$ transition operator [10–30 Weisskopf units (W.u.)]. In Fig. 1, one can see that the level with wave function $|\mathrm{rot}(2);0\rangle$ and eigenvalue $E^2(\mathrm{rot};0)$ is classified into the fourth band. Moreover, only for the lowest few levels ($i \lesssim 5$) are bands well developed and separated. For all other levels, the notation rot is just a convenient tool to classify the eigenvalues within the 2p-Cd core coupled subspace. In the following discussions (Secs. II B and III) we will use "rotational-like configuration, excitation,..." for the excitations, corresponding with the lowest bands obtained within the 2p-Cd core coupled subspace.

Finally, the wave function of Eq. (2.6) becomes

$$|i;JM\rangle = \sum c^i(NR;J)|NR;JM\rangle + \sum_j s^i[\mathrm{rot}(j)]|\,\mathrm{rot}(j);JM\rangle\,. \qquad (2.10)$$

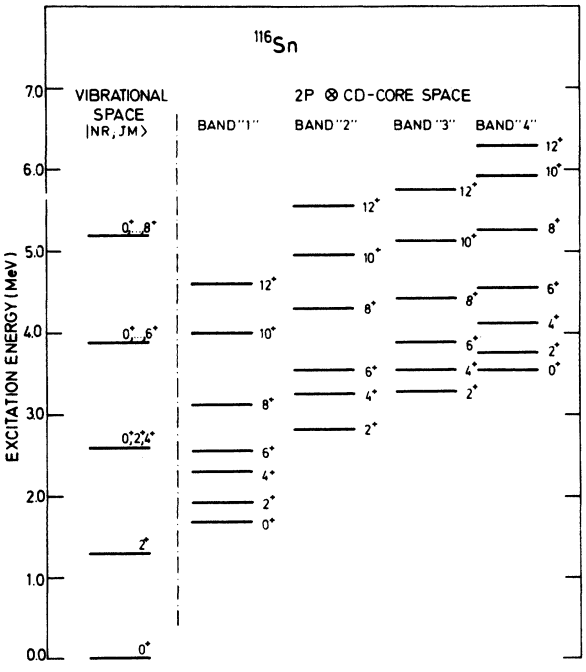

FIG. 1. For the particular nucleus ^{116}Sn, we show the unperturbed energies for the quadrupole vibrational configurations $N_2\hbar\omega_2$ as well as the energies E^i (rot ; J) obtained by solving Eq. (2.9) within the 2p-Cd core coupled configuration space (see also Sec. IIB) for the four lowest bands.

In this representation, the possible mixing of low-lying quadrupole vibrations with other collective degrees of freedom (rotational-like) is clearly expressed in terms of the amplitudes c^i and s^i.

B. Parameters and approximations

In the calculations carried out for the $^{112-118}$Sn nuclei, where most evidence for rotational-like collective bands exists, the following parameters have been used.

(i) For the nucleon-nucleon interaction $V_{\alpha\beta\gamma\delta}$, we used a surface delta interaction (SDI) force with strength fixed at $G = 25/A$ MeV.[20]

(ii) For the Coulomb interaction, only the direct term is considered, which becomes for the diagonal proton p-h configurations almost state independent and equal to −0.25 MeV. The nondiagonal term is generally small.[21] The importance of the attractive Coulomb interaction for proton 2p-2h excitations was already pointed out earlier by Flynn and Kunz,[22] since the nuclear residual p-h matrix elements give only small contributions (−0.1 MeV to 0.1 MeV).

(iii) The hole-Sn core and particle-Cd core coupling strengths ξ_2 have been obtained via a harmonic approximation[5] from known $B(E2;2_1^+ \to 0_1^+)$ values in Sn and Cd, respectively.[23] They are given in Table I, as well as the quadrupole phonon energy $\hbar\omega_2$, taken as the excitation energy $E_x(2_1^+)$ of the first excited $J^\pi = 2^+$ state.

(iv) Unperturbed values for the lowest proton 2p-2h excitations, i.e., $2[\epsilon_{1g_{7/2}}(\epsilon_{2d_{5/2}}$ for ^{112}Sn) $-\epsilon_{1g_{9/2}}]$, are taken from proton separation energies as $S_p(Z=50) - S_p(Z=51)$. The relative single-particle (-hole) energies, obtained from a recent study of odd-mass In nuclei,[5,24] are also used here (see Table I).

(v) The lowest eigenvalue $\omega(0^+,1)$, describing the binding energy of Cd with respect to the unperturbed proton 2h-Sn core system, was obtained from experimental proton separation energies [Eq. (2.5)] (see also Table I).

In order to carry out the calculations discussed above, approximations can eventually be performed. Thereby, numerical efforts are simplified without loss of the general physics content.

(i) In the first term of (A4), when calculating the contribution of $H_{p\text{-core}}$, we have the possibility of approximating the Cd eigenstates $|k;IM\rangle$ in terms of pure quadrupole collective vibrational excitations. Thereby, we impose the relation

$$|k;IM\rangle \simeq |(1g_{9/2})_{0^+}^{-2} \otimes NR;IM\rangle\delta_{RI}\,, \qquad (2.11)$$

which only holds approximately[25,26] (the rank number k is simply related with the number of quadrupole phonons N). Calculating for a limited

TABLE I. The parameters used in the present calculation (in MeV). Phonon energy $\hbar\omega_2$, coupling strength ξ_2, single-hole ($\tilde{\epsilon}_h$, defined as positive values, relative to the least bound $1g_{9/2}$ single-hole level), and single-particle energies (ϵ_p, relative to either the $1g_{7/2}$ or $2d_{5/2}$ orbital). Also, the lowest unperturbed proton 2p-2h energy $2(\epsilon_p - \epsilon_h)$ and the binding energy in the 2h-Sn core coupled system $\omega(0^+,1)$ (see also Sec. IIB) are given.

	112	114	116	118
$\hbar\omega_2$ (Sn)	1.250	1.300	1.290	1.225
$\hbar\omega_2$ (Cd)	0.657	0.617	0.558	0.514
ξ_2 (Sn)	2.3	2.0	2.0	2.0
ξ_2 (Cd)	5.9	6.7	7.5	8.5
$\tilde{\epsilon}_{2p_{1/2}}$	0.8	0.7	0.6	0.6
$\tilde{\epsilon}_{2p_{3/2}}$	1.4	1.3	1.3	1.3
$\tilde{\epsilon}_{1f_{5/2}}$	2.1	2.1	2.0	2.0
$\epsilon_{1g_{7/2}}$	0.2	0	0	0
$\epsilon_{2d_{5/2}}$	0	0.2	0.5	0.75
$\epsilon_{2d_{3/2}}$	2.6	2.6	2.6	2.6
$\epsilon_{3s_{1/2}}$	2.95	2.95	2.95	2.95
$\epsilon_{1h_{11/2}}$	2.10	2.10	2.10	2.10
$2(\epsilon_p - \epsilon_h)$	8.93 ± 0.08	9.99 ± 0.04	9.72 ± 0.05	9.76 ± 0.04
$\omega(0^+,1)$	2.19 ± 0.01	2.39 ± 0.01	2.47 ± 0.02	2.46 ± 0.02

number of K matrix elements the full contribution of $H_{\text{p-core}}$, one finds matrix elements which are on the average 10–30% larger compared with calculations imposing the constraint of only considering $(1g_{9/2})_{0^+}^{-2}$ proton 2h configurations. In these calculations, we used the parameters ξ_2 and $\hbar\omega_2$ as referred to the Sn nuclei, since $|NR;JM\rangle$ denotes the harmonic quadrupole vibrations of these nuclei. In the light of the results obtained above, we can replace the 2p-Cd core calculation by a macroscopic calculation, approximating the $|k;IM\rangle$ Cd eigenstates to pure harmonic quadrupole vibrations. Thereby we take the parameters ξ_2 and $\hbar\omega_2$ immediately from the Cd nuclei. This replacement can be carried out since the strength of the matrix element is determined by the product $\xi_2\hbar\omega_2$, which is not much different in going from Sn to Cd nuclei (in going from Sn to Cd, $\hbar\omega_2$ is lowered by a factor of 2 to 3, whereas ξ_2 grows by a factor of 3 to 4; see also Table I). Finally, in the actual calculations, use was made of this simplifed K matrix element, which becomes

$$K \simeq \langle (p_1p_2)J_p, NR; JM | V_{pp} + H_{\text{p-core}} | (p_1'p_2')J_p', N'R'; JM\rangle_{\text{Cd}} + \langle (p_1p_2)J_p(1g_{9/2})_{0^+}^{-2}; J_pM_p | V_{ph} + V_{\text{Coul}} | (p_1'p_2')J_p'(1g_{9/2})_{0^+}^{-2}; J_p'M_p'\rangle \delta_{J_pJ_p'}\delta_{M_pM_p'}, \tag{2.12}$$

where the index Cd means reference for all collective quantities to the Cd nucleus.

(ii) In calculating the L matrix elements however, the approximation of taking into account only $(1g_{9/2})_{0^+}^{-2}$ proton 2h configurations in the expansion of Cd eigenstates $|k;IM\rangle$ turns out not to be valid. Considering the most important proton 2h contributions only [i.e., pair configurations $(h)_{J_h=0}^{-2}$], the L matrix element (A2) becomes

$$L \simeq -\sum_h \alpha^h((h)_0^2, NR; R)\,\langle (p)^2; 0 | V_{pp} | (h)^2; 0\rangle, \tag{2.13}$$

where the summation index h goes over $1g_{9/2}$, $2p_{1/2}$, $2p_{3/2}$, and $1f_{5/2}$. Explicit calculation for the lowest quadrupole phonon states $|NR;JM\rangle$ were carried out. The results are independent of the particular quantum numbers p (using an SDI interaction) and are presented in Table II. Here one can see in detail that with growing angular momentum R the average coupling strength between the collective quadrupole vibrations in Sn and the 2p-Cd core coupled configurations is lowering. One also observes that the noncollective states $|k;IM\rangle$ in Cd (i.e., $J_i^\pi = 0_2^+, 6_1^+, 8_{1,2,3}^+, 10_{1,2,3,4}^+, \ldots$) couple only weakly with the quadru-

TABLE II. Calculated L matrix elements, according to Eq. (2.13). The numbers are expressed in units of $\langle (p)^2;\, 0|V_{pp}|(1g_{9/2})^2;\, 0\rangle$.

(I,k)	(N,R)	$\langle (p)_0{}^2, Ik;\, R\|V_{pp}\|NR\rangle$	(I,k)	(N,R)	$\langle (p)_0{}^2, Ik;\, R\|V_{pp}\|NR\rangle$
0_1^+	0,0	+1.10	2_3^+	3,2	+0.12
0_1^+	2,0	+0.28	2_4^+	1,2	−0.17
0_1^+	3,0	0	2_4^+	2,2	−0.50
0_2^+	0,0	+0.10	2_4^+	3,2	+0.05
0_2^+	2,0	−0.25	2_5^+	1,2	+0.12
0_2^+	3,0	−0.10	2_5^+	2,2	−0.30
0_3^+	0,0	+0.62	2_5^+	3,2	−0.20
0_3^+	2,0	−0.85	4_1^+	2,4	−0.65
0_3^+	3,0	+0.08	4_1^+	3,4	0
0_4^+	0,0	+0.08	4_2^+	2,4	−0.65
0_4^+	2,0	+0.04	4_2^+	3,4	−0.15
0_4^+	3,0	+0.50	4_3^+	2,4	−0.20
2_1^+	1,2	−0.90	4_3^+	3,4	+0.40
2_1^+	2,2	0	4_4^+	2,4	−0.10
2_1^+	3,2	−0.15	4_4^+	3,4	−0.05
2_2^+	1,2	+0.20	6_1^+	3,6	−0.15
2_2^+	2,2	+0.65	6_2^+	3,6	−0.50
2_2^+	3,2	+0.05	8_4^+	4,8	+0.30
2_3^+	1,2	+0.50	10_5^+	5,10	+0.30
2_3^+	2,2	−0.45	12_6^+	6,12	+0.20

pole vibrational states $|NR;JM\rangle$ of Sn. Therefore, and since we have in mind a description of strongly collective bands in doubly-even Sn nuclei, we have neglected such noncollective states in our calculations (as we also neglected the explicit introduction of neutron 2qp configurations). Finally, in the actual calculations, we used L matrix elements as calculated in Eq. (2.13).

Before entering into the results of these calculations for $^{112\text{-}118}$Sn, we first show the influence of the different terms of the Hamiltonian of Eq. (2.1) in a detailed way, on the $J^\pi = 0^+$ levels for ^{116}Sn (see Figs. 2 and 3). In Fig. 2, for the lowest four $J^\pi = 0^+$ levels, the energy eigenvalues from the diagonalization described in Eq. (2.9) are shown as a function of the particle-Cd core coupling strength ξ_2. In the first column of levels, the unperturbed value $\Delta E_{ph} \equiv (\epsilon_{p_1} + \epsilon_{p_2} - 2\epsilon_{1g_{9/2}}) + \omega(0^+,1)$ is given. In the next two columns (still for $\xi_2 = 0$), the contribution of, respectively, the diagonal and nondiagonal pairing and particle-hole contributions (nuclear + Coulomb) to the K matrix element are drawn [see also Eqs. (2.12) and (A2)]. Here, one can see the importance of the particle-Cd core interaction in lowering the relevant states $|\mathrm{rot}(i);JM\rangle$ near the unperturbed one-, two-, and three-quadrupole phonon states of the Sn core itself (dashed horizontal lines). In Fig. 3, the L matrix elements are incorporated, leading to final spectra, to be discussed in Sec. III. The main character of a particular level in Fig. 3 can be easily followed as a function of the coupling strength. The coupling strength ξ_2, as obtained from $B(E2; 2_1^+ \to 0_1^+)$ in the case of ^{116}Sn(^{114}Cd), becomes $\xi_2 \simeq 7.5$. From these figures, one can see in a clear way how specific correlations among the

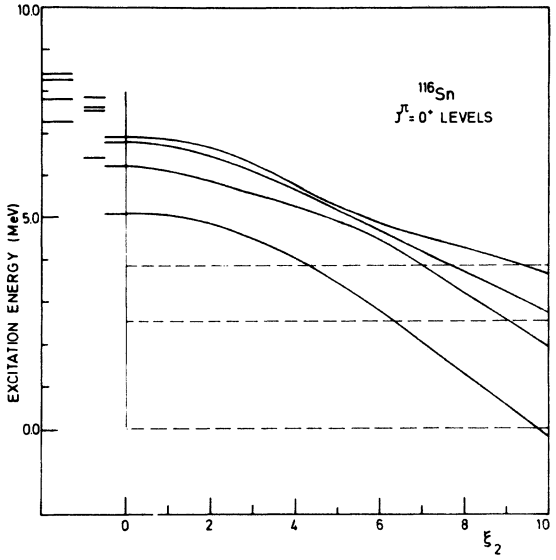

FIG. 2. The variation of the lowest four $J^\pi = 0^+$ levels in ^{116}Sn [see Eq. (2.9)] as a function of the 2p-Cd core coupling strength ξ_2 (with the L matrix elements set equal to zero). The first column shows the unperturbed proton 2p-2h energies ΔE_{ph} (see Sec. IIB). In the next two columns (still for $\xi_2 = 0$), contributions of the diagonal and nondiagonal pairing and particle-hole interactions, respectively, to the K matrix element are drawn [Eq. (2.12)]. The unperturbed, pure quadrupole vibrational configurations in Sn are shown as dashed lines.

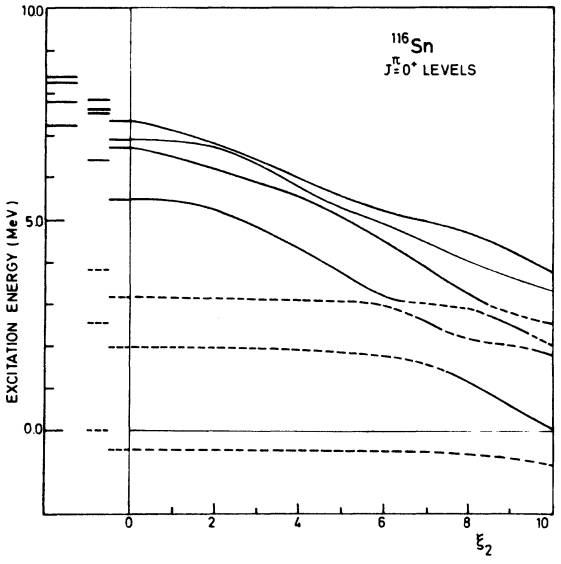

FIG. 3. Same as Fig. 2, but including the L matrix elements of Eq. (2.13). Moreover, the main character of a particular level is indicated by the structure of the line (full line: 2p-Cd configuration; dashed line: quadrupole vibration in Sn) to guide the eye.

proton 2p-2h pairs build up, via interaction with the underlying core quadrupole vibrations, and can create low-lying ($E_x \simeq 2.0$ MeV) $J^\pi = 0^+$ levels.

III. RESULTS FOR $^{112\text{-}118}$Sn

A. Energy spectra

For the most documented case, ^{116}Sn, we show in Fig. 4 the calculated level schemes, obtained for two slightly different ξ_2 values and also show the experimental data of the Amsterdam group.[9,10,27-30] In the experimental level scheme of ^{116}Sn, as well as for the other doubly-even Sn nuclei, we only show part of the total level scheme[30] since one cannot expect, by this simple model, to explain also all the explicit neutron

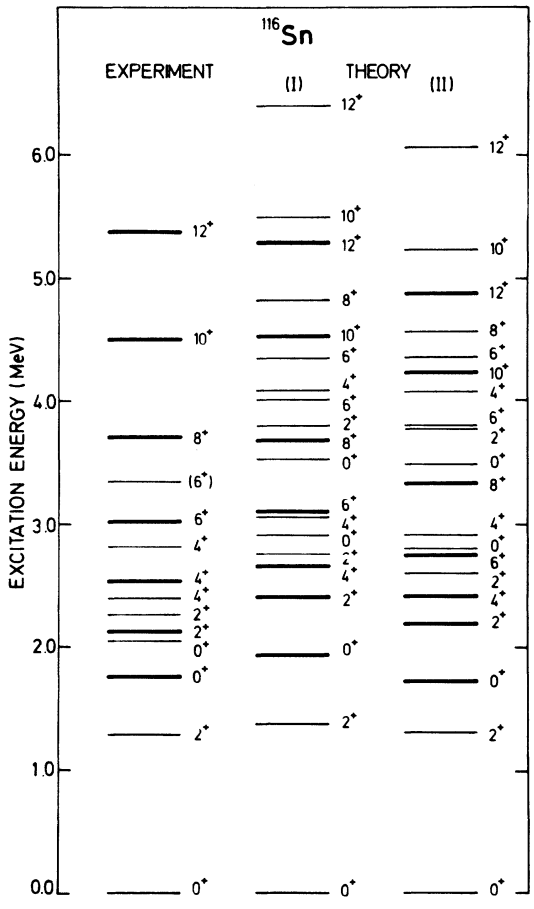

FIG. 4. Comparison of experimental (Refs. 27–30) and calculated [(I) and (II) correspond with $\xi_2 = 7.5$ and 8.0, respectively] level schemes for ^{116}Sn. The thick lines indicate levels which contain most of the 2p-Cd core coupled configuration space. Experimentally, only part of the levels are drawn (neglect of explicit neutron 2qp levels; see Ref. 30).

2qp degrees of freedom. Moreover, for the theoretical results, only the lowest bands are shown. More complete results (energies, wave function, etc.) can be obtained on request from the authors. As can be seen, the experimentally observed rotational-like band is well described starting from the proton 2p-Cd core configurations, interacting by means of the strong residual particle-Cd core coupling as well as through mixing with the underlying (idealized) quadrupole vibrational excitations of the Sn core. The wave functions corresponding to the lowest $J^\pi = 0^+$, 2^+, 4^+ and 6^+ levels (for $\xi_2 = 7.5$) are given in Table III. Here, we use the expansion of the wave function as explained in Eq. (2.10) since within this particular representation, the smallest number of configurations is needed to express most of the total wave function. Inspecting these wave functions, it becomes clear that one cannot talk of coexistence between two modes of motion—vibrational and rotational-like—but that rather strong mixing for the $J_i^\pi = 0^+_{2,3}, 2^+_{2,3}, 4^+_{1,2}$ levels results. For these particular levels, it is difficult to make a clear-cut difference judging on their most important amplitude. Later on, in calculating the $E2$ and $E0$ decay properties, peculiar experimental data will show up that ask for such important admixtures in the wave functions, corresponding with both the $J_i^\pi = 0_2^+$ and 0_3^+ levels.

One can therefore, in the light of the present calculations and the recent experimental data[27-34] on ^{116}Sn, conclude that a more complicated situation than just coexistence of vibrational, neutron 2qp, and rotational-like degrees of freedom exists.

In Fig. 5 we show the results obtained for ^{112,114,118}Sn, respectively. Again, the experimental data result from the extensive work of the Amsterdam group.[27-30] In these figures, besides the full diagonalization, we show the unperturbed energies corresponding to harmonic quadrupole vibrations and the energy spectrum of the lowest band within the 2p-Cd core coupled states [see Eqs. (2.8) and (2.9)]. In both the experimental and theoretical results, we indicate with a thick line the levels which contain most of the proton 2p-Cd core configuration space. As already pointed out before, especially for the $J_i^\pi = 0^+_{2,3}$, $2^+_{2,3}$, and $4^+_{1,2}$ levels, this separation is not always very clear cut. Also, one observes that in most Sn nuclei, three (four in ^{112}Sn) low-lying $J^\pi = 4^+$ levels result, which probably can be classified as admixtures of neutron 2qp, vibrational, and proton 2p-Cd core coupled configurations. Due to the very schematic structure of our model space, oversimplifications are introduced such that detailed comparison for all low spin ($J^\pi \lesssim 4^+$) states

TABLE III. Wave functions for the $J_i^\pi = 0^+_{1,2,3,4}$, $2^+_{1,2,3,4}$, $4^+_{1,2,3}$, and $6^+_{1,2}$ levels in ^{116}Sn for a coupling strength of $\xi_2 = 7.5$. The wave function is expressed in the representation given by Eq. (2.10).

$$|0_1^+\rangle = 0.94\,|00;0\rangle + 0.25\,|\mathrm{rot}(1);0\rangle - 0.07\,|\mathrm{rot}(2);0\rangle$$

$$|0_2^+\rangle = 0.17\,|00;0\rangle - 0.61\,|20;0\rangle - 0.74\,|\mathrm{rot}(1);0\rangle$$

$$|0_3^+\rangle = -0.15\,|00;0\rangle - 0.68\,|20;0\rangle - 0.13\,|30;0\rangle + 0.61\,|\mathrm{rot}(1);0\rangle + 0.08\,|\mathrm{rot}(2);0\rangle$$

$$|0_4^+\rangle = 0.11\,|20;0\rangle - 0.81\,|30;0\rangle - 0.12\,|\mathrm{rot}(1);0\rangle - 0.20\,|\mathrm{rot}(2);0\rangle$$

$$|2_1^+\rangle = 0.89\,|12;2\rangle - 0.02\,|22;2\rangle + 0.02\,|32;2\rangle - 0.38\,|\mathrm{rot}(2);2\rangle - 0.12\,|\mathrm{rot}(2);2\rangle$$

$$|2_2^+\rangle = -0.20\,|12;2\rangle - 0.65\,|22;2\rangle + 0.05\,|32;2\rangle - 0.60\,|\mathrm{rot}(1);2\rangle + 0.36\,|\mathrm{rot}(2);2\rangle + 0.09\,|\mathrm{rot}(3);2\rangle$$

$$|2_3^+\rangle = -0.30\,|12;2\rangle + 0.53\,|22;2\rangle + 0.13\,|32;2\rangle - 0.69\,|\mathrm{rot}(1);2\rangle - 0.29\,|\mathrm{rot}(2);2\rangle$$

$$|2_4^+\rangle = -0.08\,|12;2\rangle - 0.38\,|22;2\rangle + 0.15\,|32;2\rangle + 0.06\,|\mathrm{rot}(1);2\rangle - 0.84\,|\mathrm{rot}(2);2\rangle$$

$$|4_1^+\rangle = -0.63\,|24;4\rangle + 0.03\,|34;4\rangle - 0.75\,|\mathrm{rot}(1);4\rangle + 0.17\,|\mathrm{rot}(2);4\rangle$$

$$|4_2^+\rangle = -0.67\,|24;4\rangle - 0.06\,|34;4\rangle + 0.65\,|\mathrm{rot}(1);4\rangle + 0.29\,|\mathrm{rot}(2);4\rangle$$

$$|4_3^+\rangle = -0.28\,|24;4\rangle + 0.16\,|34;4\rangle + 0.08\,|\mathrm{rot}(1);4\rangle - 0.91\,|\mathrm{rot}(2);4\rangle$$

$$|6_1^+\rangle = -0.05\,|36;6\rangle + 0.99\,|\mathrm{rot}(1);6\rangle$$

$$|6_2^+\rangle = -0.37\,|36;6\rangle + 0.03\,|\mathrm{rot}(1);6\rangle - 0.93\,|\mathrm{rot}(2);6\rangle$$

$$|6_3^+\rangle = -0.63\,|36;6\rangle + 0.30\,|\mathrm{rot}(1);6\rangle$$

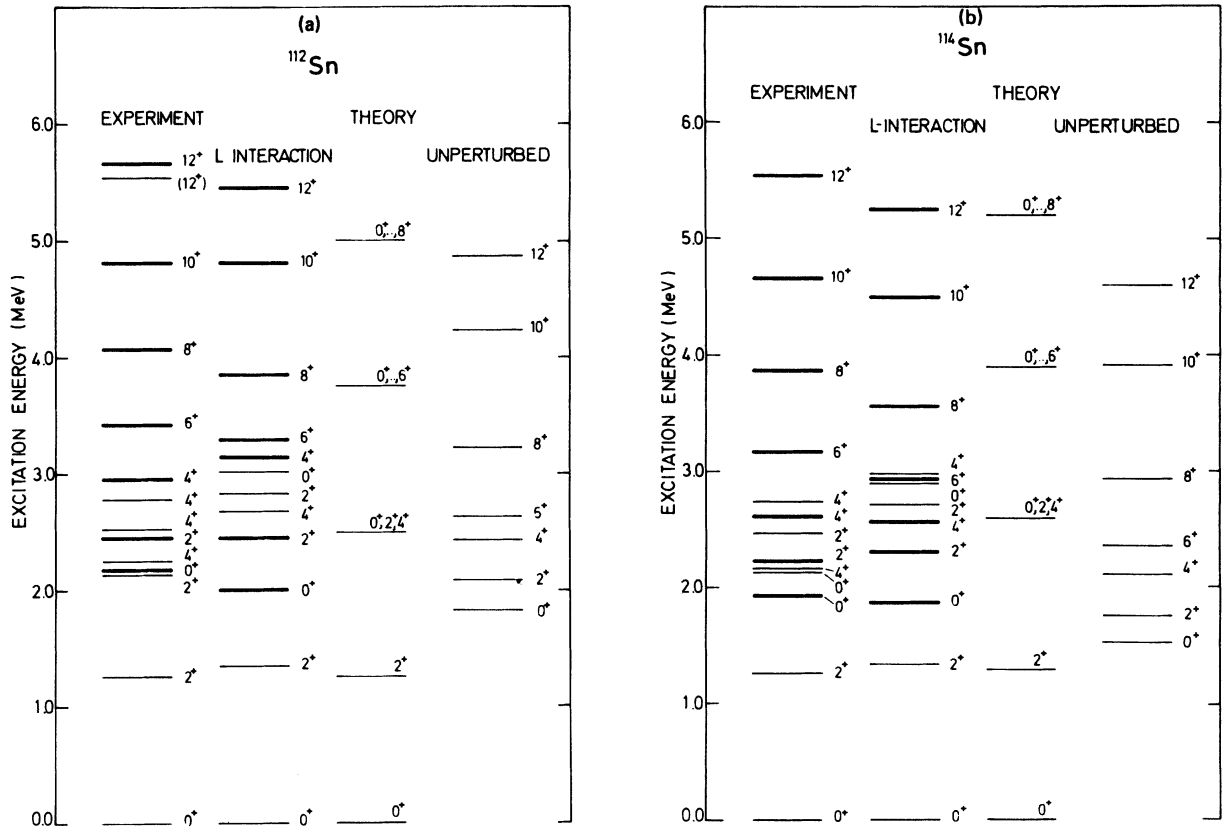

FIG. 5. Comparison of experimental (Refs. 27–30) and calculated level schemes for (a) ^{112}Sn, (b) ^{114}Sn, and (c) ^{118}Sn. Thick lines indicate levels containing most of the 2p-Cd core coupled configuration space. Besides the full diagonalization [Eq. (2.7)], we also show the unperturbed energies corresponding with harmonic quadrupole vibrations and with the lowest band $E^1(\mathrm{rot};J)$ [see Eq. (2.9)] with in the 2p-Cd core coupled configuration space.

is not possible; however, the main feature studied here—the description of collective rotational-like bands—seems quite possible.

B. $E2$ and $E0$ decay properties

Extra tests on the structure of the wave functions, as obtained here, can be carried out by calculating electromagnetic decay properties. Since extensive studies on $E2$ and $E0$ decay have been carried out recently,[31-34] we will concentrate on these particular interesting decay modes.

The standard $E2$ transition operator, containing both single-particle $[\mathfrak{M}(E2)_{\mathrm{sp}}]$ and collective vibrational contributions $[\mathfrak{M}(E2)_{\mathrm{coll}}]$, has been used throughout.[5,35] As the proton effective charge, we use $e_p^{\mathrm{eff}} = 1.5e$ and the experimental $B(E2; 2_1^+ \to 0_1^+)$ values for Sn and Cd nuclei determine the collective transition strength. Working in the basis of Eq. (2.6), one gets as the reduced $E2$ matrix element

$$\begin{aligned}\langle J_f \| \mathfrak{M}(E2) \| J_i \rangle = & \sum_{N,R,N',R'} c^i(NR;J_i)c^f(N'R';J_f)\langle N'R' \| \mathfrak{M}(E2)_{\mathrm{coll}} \| NR \rangle \\ & + \sum_{\{O_i,O_f\}} l^i((\mathrm{p}_1\mathrm{p}_2)J_{\mathrm{p}}, Ik; J_i) l^f((\mathrm{p}_1'\mathrm{p}_2')J_{\mathrm{p}}', I'k'; J_f)\hat{J}_f\hat{J}_i(-1)^{I+J_{\mathrm{p}}'} \\ & \times \left\{ \begin{matrix} J_{\mathrm{p}}' & J_f & I \\ J_i & J_{\mathrm{p}} & 2 \end{matrix} \right\} (-1)^{J_i} \langle (\mathrm{p}_1'\mathrm{p}_2')J_{\mathrm{p}}' \| \mathfrak{M}(E2)_{\mathrm{sp}} \| (\mathrm{p}_1\mathrm{p}_2)J_{\mathrm{p}} \rangle \delta_{II'}\delta_{kk'} \\ & + \left\{ \begin{matrix} I' & J_f & J_{\mathrm{p}}' \\ J_i & I & 2 \end{matrix} \right\} (-1)^{J_f} D(\mathrm{p}_1'\mathrm{p}_2', \mathrm{p}_1\mathrm{p}_2; J_{\mathrm{p}}) [(1+\delta_{\mathrm{p}_1\mathrm{p}_2})(1+\delta_{\mathrm{p}_1'\mathrm{p}_2'})]^{-1/2} \langle I'k' \| \mathfrak{M}(E2)_{\mathrm{coll}} \| Ik \rangle \Bigg) , \quad (3.1)\end{aligned}$$

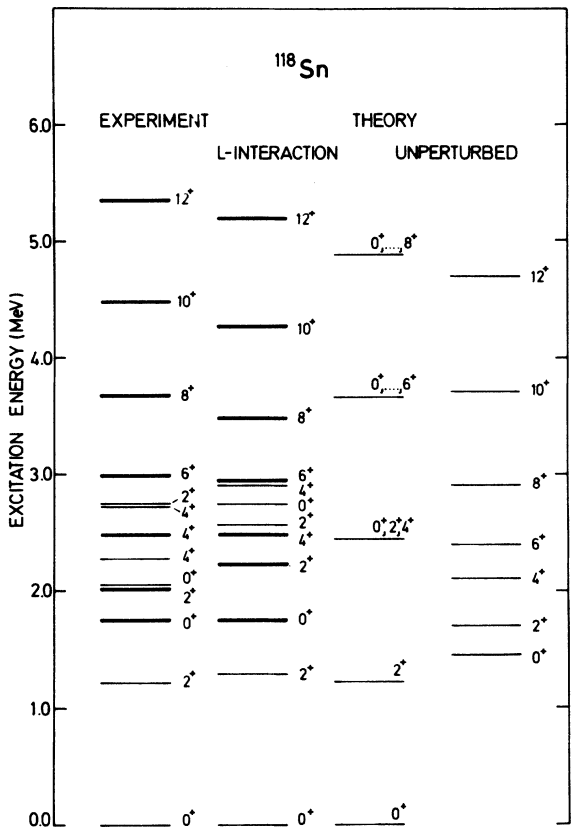

FIG. 5 *(Continued)*.

Here, $D(ab,cd,J)$ is a notation for $\delta_{ac}\cdot\delta_{bd} - (-1)^{j_a+j_b-J}\delta_{ad}\cdot\delta_{bc}$. Furthermore, the single-particle reduced $E2$ matrix element is calculated between normalized, antisymmetrized 2p states and we use the notation $\{O_i, O_f\}$ for summation over all quantum numbers occuring in the expansion coefficients l^i and l^f. In line with approximation (i), discussed in Sec. II, to simplify the states $|k;IM\rangle$ in Cd by harmonic quadrupole vibrational excitations, one can now approximate the collective $E2$ matrix elements $\langle I'k'\|\mathfrak{M}(E2)_{\rm coll}\|Ik\rangle$ as being defined with respect to Cd core matrix elements. The latter assumption is very plausible since the proton 2h system [for Sn and Cd, where the pairing energy $\Delta_{1g_{9/2}} > \hbar\omega_2(\mathrm{Sn})$] interferes in such a way with the collective $E2$ transition rate in the Sn nucleus to induce coherence.[36] For ^{114}Cd, with an experimental reduced $E2$ transition probability $B(E2;2_1^+\to 0_1^+) = 10.6\pm0.1\ e^2b^2\times10^{-2}$ (Ref. 23), the explicit calculation yields $9.8\ e^2b^2\times10^{-2}$ although the $B(E2;2_1^+\to 0_1^+)$ value for ^{116}Sn only amounts to $4.3\pm0.1\ e^2b^2\times10^{-2}$.

The $E0$ operator reads [35,37,38]

$$\mathfrak{M}(E0) = \sum_i e_i r_i^2 + k\sum_\mu |\alpha_\mu|^2 , \tag{3.2}$$

where the collective contribution with respect to quadruople vibrations, can be rewritten as

$$\mathfrak{M}(E0)_{\rm coll} = k\hbar\omega_2/(2C_2)\sum_\mu \left[b_{2,\mu}b^\dagger_{2,\mu} + b^\dagger_{2,-\mu}\,b_{2,-\mu} + (-1)^\mu b_{2,\mu}b_{2,-\mu} + (-1)^\mu b^\dagger_{2,-\mu}b^\dagger_{2,\mu}\right], \tag{3.3}$$

Here, we use the estimate for $k \simeq (3/4\pi)\,ZeR_0^2$ (Ref. 37).

Moreover, the parameter $\hbar\omega_2/(2C_2)$ is related, within a harmonic quadrupole vibrator model, with the value $B(E2;\ 2_1^+\to 0_1^+)$.[39] The necessary collective matrix elements are easily calculated as

$$\langle NR\,|\mathfrak{M}(E0)_{\rm coll}\,|NR\rangle = (N+\tfrac{5}{2})k\hbar\omega/C_2 , \tag{3.4}$$

$$\langle NR\,|\mathfrak{M}(E0)_{\rm coll}\,|N-2,R\rangle = \sum_{R'}\langle NR\|b_2^\dagger\|N-1,R'\rangle\langle N-1,R'\|b_2^\dagger\|N-2,R\rangle(-1)^{R+R'}\{1/[2(2R+1)]\}(k\hbar\omega_2/C_2) . \tag{3.5}$$

Here, $\langle\cdots\|b_2^\dagger\|\cdots\rangle$ denotes boson reduced matrix elements which are related to quadrupole boson coefficients of fractional parentage (cfp's).[40] They have been calculated, using the method of Sau *et al.*,[41] but applied for bosons. The final result for the total $E0$ matrix element [using the expression (2.6) for the nuclear wave functions with the restriction of only $(1g_{9/2})_{0^+}^{-2}$ 2h configurations] becomes

$$\begin{aligned}\langle J_f\|\mathfrak{M}(E0)\|J_i\rangle = {} & \sum_{N,R,N',R'} c^i(NR;J_i)c^f(N'R';J_f)\langle N'R'\|\mathfrak{M}(E0)_{\rm coll}\|NR\rangle\,\delta_{NN'}\,\delta_{RR'} \\ & + \sum_{\substack{\{O_i,O_f\}\\ N',N'',R''}} l^i((p_1p_2)J_p, Ik; J_i)l^f((p_1'p_2')J_p', I'k'; J_f)(2J_i+1) \\ & \times\{(\hat J_p\hat J_i)^{-1}[\langle p_1'\|\mathfrak{M}(E0)_{sp}\|p_1\rangle - \langle 1g_{9/2}\|\mathfrak{M}(E0)_{sp}\|1g_{9/2}\rangle] \\ & \times(1+\delta_{p_1p_2})\delta_{p_1'p_1}\delta_{p_2'p_2}\delta_{J_p'J_p}\delta_{I'I}\delta_{k'k} + (\hat R''\hat J_i)^{-1}\langle N''R''\|\mathfrak{M}(E0)_{\rm coll}\|N'''R''\rangle \\ & \times D(p_1'p_2', p_1p_2; J_p)[(1+\delta_{p_1p_2})(1+\delta_{p_1'p_2'})]^{-1/2}\,\delta_{R''I}\delta_{R'''I'}\delta_{J_p'J_p}\} . \end{aligned} \tag{3.6}$$

In expression (3.6), the quadrupole vibrational states always refer to the Sn-core nucleus, because we explicitly expanded the $|k;IM\rangle$ Cd core states into its proton 2h-Sn core components [see Eq. (2.4)], only taking into account $(1g_{9/2})_{0^+}{}^{-2}$ configurations. In further discussing the $B(E0)$ rates, two quantities are very often used to enable easy comparison with the experimental data[31-34]:

$$\rho^2 \equiv B(E0)/e^2R_0{}^4 \quad (R_0 \text{ is the nuclear radius}), \tag{3.7}$$

$$X_{i,f} \equiv B(E0; 0_i^+ \rightarrow 0_f^+)/B(E2; 0_i^+ \rightarrow 2_1^+) \, . \tag{3.8}$$

For a harmonic quadrupole vibrator, taking $J_i^\pi = 0_i^+$ as the first excited 0_2^+, two phonon state, one easily obtains for the ratio

$$X_{2,1} = \beta^2 \, . \tag{3.9}$$

This $X_{2,1}$ value, also called the spherical vibrator value, will be mainly used as a reference value in discussing the $E0$ properties of excited $J^\pi = 0^+$ levels in doubly-even Sn nuclei. First of all, in discussing the results, we give in Table IV for the low-lying levels on ^{116}Sn and for two different ξ_2 values, calculated $B(E2)$ values and compare with the recent experimental data of Bäcklin *et al.*[32] The resulting values are given in W.u. As already discussed in Sec. III A, a unique location of the vibrational, neutron 2qp, and rotational-like features of the experimental spectrum is very difficult. Therefore we will mainly concentrate, in the discussion, on the $J^\pi = 0^+$ and 2^+ levels in $^{112-118}$Sn. For the $J^\pi = 0^+$ levels, the value of $B(E2; 0_3^+ \rightarrow 2_1^+)$ is only 0.5 W.u., which is in striking contrast to the corresponding $E2$ transition from the $J_i^\pi = 0_2^+$ level [$B(E2; 0_2^+ \rightarrow 2_1^+) = 17$ W.u.]. By inspecting the $J_i^\pi = 0_{2,3}^+$ and 2_1^+ wave functions of Table II, this can qualitatively be understood as an *interference effect between the vibrational and rotational-like E2 transition amplitudes*. Since $|0_2^+\rangle$ and $|0_3^+\rangle$ are orthogonal combinations of mainly two configurations, i.e., $|20;0\rangle$ and $|\text{rot}(1);0\rangle$, both decaying to the one-quadrupole phonon $J_f^\pi = 2_1^+$ level (mainly $|12;2\rangle$ with an admixture of $-0.4\,|\text{rot}(1);2\rangle$), these experimental facts can easily be understood. Exactly the same argument will apply in explaining the particular strong $0_3^+ \rightarrow 0_2^+$ and weak $0_3^+ \rightarrow 0_1^+$ $E0$ decay rates.

The $E2$ decay of the $J_i^\pi = 2_2^+$ level, which probably is the experimental level containing most of the rotational-like configurations, is generally well described. Both the $2_2^+ \rightarrow 0_2^+$ and $2_2^+ \rightarrow 0_3^+$ $E2$ transition probabilities are large,[31-34] a fact that is well described theoretically but cannot easily be understood relying on vibrational and neutron 2qp degrees of freedom only. In the decay of the $J_i^\pi = 2_3^+$ level, some large deviations between theory and experiment occur, which are probably due to a too strong mixing of both the vibrational and rotational-like $J^\pi = 2^+$ configurations.

TABLE IV. Comparison of calculated [(I) and (II) correspond with a coupling strength $\xi_2 = 7.5$ and 8.0, respectively] and very recent experimental $B(E2)$ values in ^{116}Sn (Ref. 32).

	$B(E2)$ (W.u.)		
	Theory		
$J_i^\pi \rightarrow J_f^\pi$	(I)	(II)	Experiment[a]
$2_1^+ \rightarrow 0_1^+$	15.1	15.7	13
$2_2^+ \rightarrow 0_1^+$	0.03	0.12	0.06
$\rightarrow 0_2^+$	7.1	18	26
$\rightarrow 0_3^+$	8.9	12.2	32
$\rightarrow 2_1^+$	26.8	23	4
$2_3^+ \rightarrow 0_1^+$	0.014	0.0007	0.05
$\rightarrow 0_2^+$	23.7	15.7	0.7
$\rightarrow 0_3^+$	13.1	4.1	<2
$\rightarrow 2_1^+$	7.0	18.1	5
$\rightarrow 2_2^+$	14.7	7.9	<3
$0_2^+ \rightarrow 2_1^+$	46.5	65.8	17
$0_3^+ \rightarrow 2_1^+$	0.67	0.99	0.5
$4_1^+ \rightarrow 2_1^+$	6.6	16.1	23
$\rightarrow 2_2^+$	12.5	11.3	60
$\rightarrow 2_3^+$	13	0.3	<2
$4_2^+ \rightarrow 2_1^+$	27.4	24.5	<0.003
$\rightarrow 2_2^+$	7.0	27	>17
$\rightarrow 2_3^+$	17.3	15.8	>0.3
$\rightarrow 4_1^+$	15.4	11.3	

[a] Reference 32.

In order to locate the $J^\pi = 4^+$ level, which contains the largest fraction of the rotational-like configurations, again difficulties arise because of large mixing. Experimentally, both the $J_i^\pi = 4_1^+$ and 4_2^+ levels are strongly connected with the $J_f^\pi = 2_2^+$ level, however, only the $J_i^\pi = 4_2^+$ level decays very weakly towards the $J_f^\pi = 2_1^+$ level, a fact that cannot be reproduced theoretically. This again points towards a somewhat too strong mixing of the vibrational and rotational-like configurations. Moreover, three $J^\pi = 4^+$ levels occur in the relevant region of mixing[31,32] and thus the neglect of neutron 2qp configurations as well as the simplifications of only considering $|k;IM\rangle$ Cd eigenstates that resemble quadrupole vibrational excitations will definitely influence calculations in the model space as used here.

In Figs. 6–8 we also show the systematic behav-

ior of $E2$ reduced transition probabilities (in units of $e^2b^2\times10^{-2}$) for the $J_i^\pi = 0^+_{2,3}$ and $2^+_{2,3}$ levels[31-34] in doubly-even $^{112-118}$Sn. The systematic interference effects for producing large $B(E2; 0^+_2 \to 2^+_1)$ and small $B(E2; 0^+_3 \to 2^+_1)$ is well described theoretically, although a detailed inspection still shows discrepancies of a factor of 3 (Fig. 6). For the weak transitions, $B(E2; 2^+_2 \to 0^+_1)$ is better described than the $B(E2; 2^+_3 \to 0^+_1)$ values (Fig. 7). For the strong reduced transition probabilities (Fig. 8), the $2^+_3 \to 2^+_1$ transition is well described but the $2^+_2 \to 2^+_1$ is calculated too fast (probably due to too strong mixing between the unperturbed, low-lying $J^\pi = 2^+$ configurations).

Concentrating now in some detail on the peculiar $E0$ decay from the excited $J_i^\pi = 0^+_{2,3}$ levels (see Figs. 9 and 10), the dominant $E0$ transition rate results from the $0^+_3 \to 0^+_2$ transition. As also discussed by Bäcklin *et al.*,[31-34] strong mixing of two states with different deformation is needed to explain these peculiar strong $E0$ transitions.

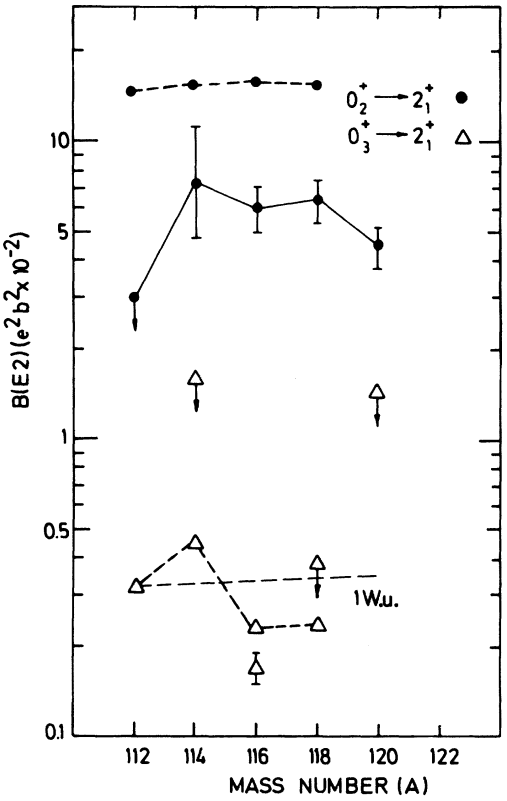

FIG. 6. Comparison of theoretical and experimental (Refs. 32, 34) $B(E2; 0^+_{2,3} \to 2^+_1)$ values as a function of the atomic mass number in doubly-even Sn nuclei ($112 \leq A \leq 120$). The experimental points are connected with a *full* line (to guide the eye) if possible, whereas the theoretical points are connected with *dashed* lines. The Weisskopf $E2$ unit (1 W.u.) is also shown for comparison (light dashed line).

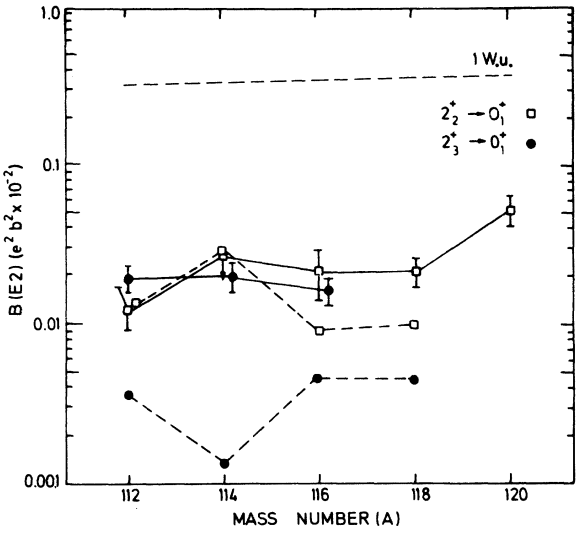

FIG. 7. Same as Fig. 6 but for $B(E2; 2^+_{2,3} \to 0^+_1)$.

Support for this interpretation also comes from a recent measurement of the ratio $B(E2; 2^+_2 \to 0^+_3)/B(E2; 2^+_2 \to 0^+_2) = 1.3 \pm 0.5$ (Ref. 32) in ^{116}Sn. (Theory gives for this ratio 1.25 and 0.7 for $\xi_2 = 7.5$ and 8.0, respectively.) From this number, one was able to deduce that $\simeq 55\%$ of the rotational-like configuration should be contained in the $J_i^\pi = 0^+_3$ level and 45% in the $J_i^\pi = 0^+_2$ level, which is in very good agreement with the calculated wave functions of Table II. Thus the arguments of strong mixing, outlined above and discussed at some length in Ref. 31, become confirmed by our more detailed calculations. Theoretically, one cannot fully describe the neutron number dependence of $B(E0)$ (ρ^2) values so well. [The theoretical $B(E0; 0^+_2 \to 0^+_1)$

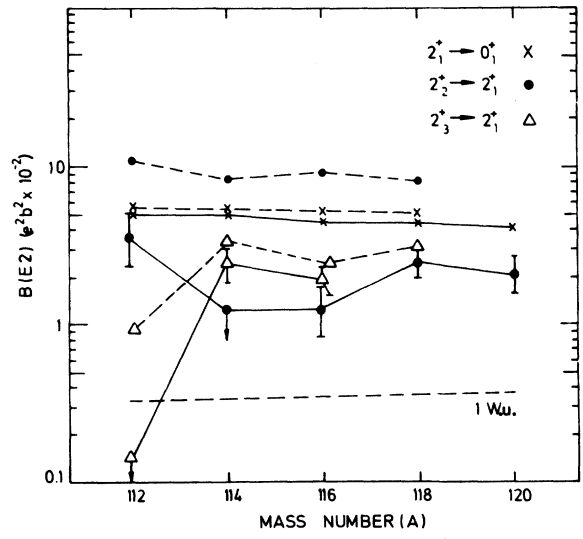

FIG. 8. Same as Fig. 6, but for $B(E2; 2^+_1 \to 0^+_1)$ and $B(E2; 2^+_{2,3} \to 2^+_1)$.

is also large in $^{112-118}$Sn whereas, experimentally, from ^{116}Sn on, much lower values are obtained.] (See Fig. 9.) Concerning the X values, we note a clustering of both $X_{2,1}$ and $X_{3,1}$ around the spherical vibrator value of 0.013 ($\beta_{Sn}{}^2$). The experimental value for $X_{3,2}$ is much larger than the spherical vibrator value which is also shown by the calculation (Fig. 10). Even the mass dependence is rather well described in this particular case.

IV. CONCLUSION

In this study, we have tried to point out the importance of proton 2p-2h excitations through the $Z = 50$ closed proton shell, in order to describe the recently observed, strong collective bands in doubly-even $^{112-118}$Sn nuclei. Within a simple model, containing proton 2p-2h excitations interacting with quadrupole vibrational excitations of the underlying Sn core, we were able to show how one can generate rotational-like bands with spin $\Delta J = 2$ sequence. Although for the lower spin members rather mixed wave functions occur, the very regular energy spacings reminiscent of rotational bands still exist. Moreover, $E2$ and $E0$ transition probabilities were calculated and extensively compared with the recent experimental data. When concentrating on the lower $J^\pi = 0^+$ and 2^+ levels, some very peculiar features [large ratio of $B(E2; 0_2^+ \to 2_1^+)/B(E2; 0_3^+ \to 2_1^+)$ and strong $B(E0; 0_3^+ \to 0_2^+)$ transition rate] could be explained via constructive and destructive interference of the two basic configurations contained in the model space: quadrupole vibrational and 2p-Cd core coupled rotational-like excitations. In the detailed comparison between experiment and theory, substantial deviations still occur.

This is probably due to the explicit neglect of neutron 2qp configurations and the restriction of Cd eigenstates $|k; IM\rangle$ to only pure quadrupole vibrational states, deleting all the noncollective ones. Also, in the particular cases of $J^\pi = 2^+_{2,3}$, $4^+_{1,2}$, too strong mixing of vibrational and rotational-like configurations occurs. Besides these shortcomings, we can summarize that the main features of doubly-even Sn nuclei could find a simple explanation.

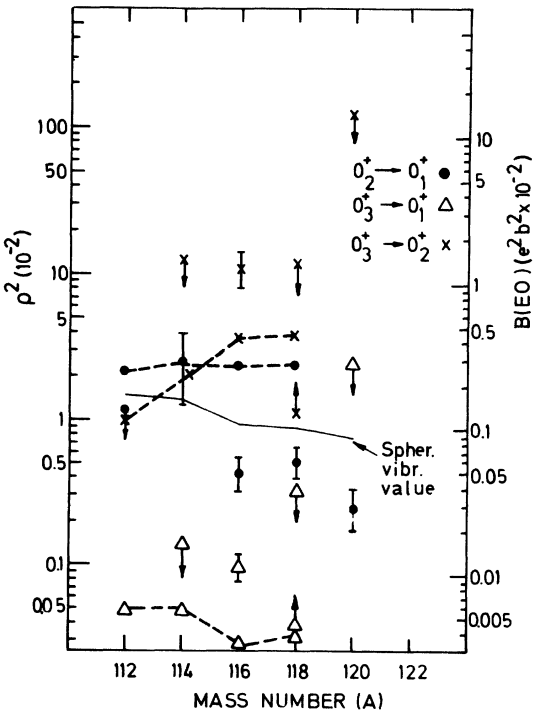

FIG. 9. The theoretical and experimental (Ref. 32) $B(E0)$ (and ρ^2) values as a function of atomic mass number for doubly-even Sn nuclei ($112 \leq A \leq 120$). Theoretical points are connected with a dashed line. The spherical vibrator value is also shown (light full line).

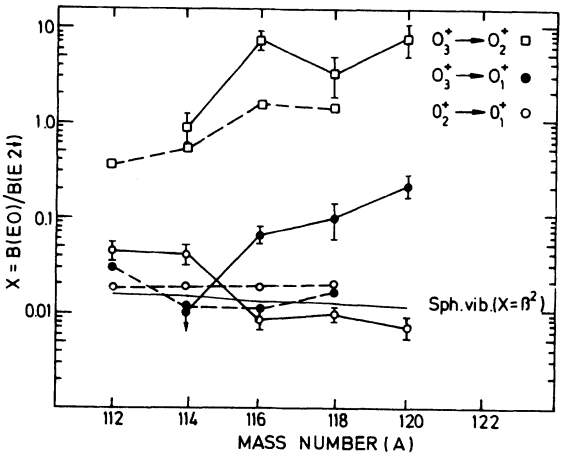

FIG. 10. The theoretical and experimental (Ref. 32) $X_{3,2}$, $X_{2,1}$, and $X_{3,1}$ values. Experimental points are connected with full lines to guide the eye and theoretical points with a dashed line. Also the spherical vibrator value for $X[=\beta^2$; see also Eq. (3.9)] is indicated with a light full line.

ACKNOWLEDGMENTS

The authors are most grateful to Prof. A. J. Deruytter for his interest during the course of this work. Two of the authors (M. W. and P. V. I.) are indebted to the NFWO and G. W. to the IWONL for financial support. One of the authors (K. H.) is much indebted to Dr. A. Bäcklin, Dr. R. Casten, and Dr. W. Hesselink for many stimulating discussions and the use of results prior to publication.

APPENDIX

The L matrix element, as used in the secular Eq. (2.7), defined as

$$L((p_1p_2)J_p, Ik; N'R'; J) \equiv \langle (p_1p_2)J_p, Ik; JM|H|N'R'; JM\rangle, \tag{A1}$$

becomes in explicit form

$$L = -\sum_{\{O\}} (-1)^{J_p+R+I}(\hat{I}/\hat{R})a^k((h_1h_2)J_h, NR; I)\langle p_1p_2; J_pM_p|V_{pp}|h_1h_2; J_pM_p\rangle\, \delta_{J_hJ_p}\delta_{NN'}\,\delta_{RR'}. \tag{A2}$$

Here, the summation indices $\{h_1, h_2, J_h, N, R\}$ are denoted in shorthand notation as $\{O\}$.

The K matrix element, defined as

$$K((p_1p_2)J_p, Ik; (p_1'p_2')J_p', I'k'; J) \equiv \langle (p_1p_2)J_p, Ik; JM|H|(p_1'p_2')J_p', I'k'; JM\rangle, \tag{A3}$$

becomes in explicit form

$$\begin{aligned} K = {} & \langle (p_1p_2)J_p, Ik; JM|V_{pp} + H_{p\text{-core}}|(p_1'p_2')J_p', I'k; JM\rangle \\ & + \sum_{\{O,O'\},\mathcal{J}} a^k((h_1h_2)J_h, NR; I)\, a^{k'}((h_1'h_2')J_h', N'R'; I')\hat{I}'\,!\,\hat{I}(2\mathcal{J}+1) \\ & \times \langle (p_1p_2)J_p(h_1h_2)J_h; \mathcal{J}\mathfrak{M}|V_{ph} + V_{Coul}|(p_1'p_2')J_p'(h_1'h_2')J_h'; \mathcal{J}\mathfrak{M}\rangle \begin{Bmatrix} J_h & R & I \\ J & J_p & \mathcal{J} \end{Bmatrix} \begin{Bmatrix} J_h' & R' & I' \\ J & J_p' & \mathcal{J} \end{Bmatrix} \delta_{NN'}\delta_{RR'}. \end{aligned} \tag{A4}$$

In Eqs. (A2) and (A4), we use the notation V_{pp}, V_{ph} for the residual nuclear particle-particle and particle-hole interactions, respectively, whereas $H_{p\text{-core}}$ describes the particle-quadrupole core interaction term [third term of the Hamiltonian H of Eq. (2.1)].

[1] W. F. Van Gunsteren, Ph.D. thesis, Vrije Universiteit, Amsterdam, 1976 (unpublished).
[2] W. F. Van Gunsteren, E. Boeker, and K. Allaart, Z. Phys. 267, 87 (1974).
[3] W. Dietrich, A. Bäcklin, C. O. Lannergard, and I. Ragnarsson, Nucl. Phys. A253, 429 (1975).
[4] K. Heyde, M. Waroquier, P. Van Isacker, and H. Vincx, Nucl. Phys. A292, 237 (1977).
[5] K. Heyde, M. Waroquier, and R. A. Meyer, Phys. Rev. C 17, 219 (1978).
[6] A. K. Gaigalas, R. E. Shroy, G. Schertz, and D. B. Fossan, Phys. Rev. Lett. 35, 555 (1977).
[7] J. Bron, W. H. A. Hesselink, H. Bedet, H. Verheul, and G. Vanden Berghe, Nucl. Phys. A279, 365 (1977).
[8] P. Van Isacker, M. Waroquier, H. Vincx, and K. Heyde, Nucl. Phys. A292, 125 (1977).
[9] J. Bron, W. H. A. Hesselink, L. K. Peker, A. Von Poelgeest, J. Uitzinger, H. Verheul, and J. Zalmstra, J. Phys. Soc. Jpn. Suppl. 44, 513 (1978).
[10] J. Bron, Ph.D. thesis, Vrije Universiteit, Amsterdam, 1978 (unpublished).
[11] R. A. Meyer and L. Peker, Z. Phys. A 283, 379 (1977).
[12] H. W. Fielding, R. E. Anderson, C. D. Zafiratos, D. A. Lind, F. E. Cecil, H. H. Wieman, and W. P. Alford, Nucl. Phys. A281, 389 (1977).
[13] K. Heyde and P. J. Brussaard, Nucl. Phys. A104, 81 (1967).
[14] V. Paar, Nucl. Phys. A211, 29 (1973).
[15] G. Alaga, *Nuclear Structure and Nuclear Reactions*, edited by M. Jean and R. A. Ricci (Academic, New York, 1969), p. 28.
[16] G. Alaga, F. Krmpotic, and V. Lopac, Phys. Lett. 24B, 537 (1967).
[17] G. Alaga, V. Paar, and V. Lopac, Phys. Lett. 43B, 459 (1973).
[18] V. Paar and R. A. Meyer, J. Phys. B 5, L75 (1979).
[19] A. H. Wapstra and K. Bos, At. Data Nucl. Data Tables 19, 177 (1977).
[20] L. S. Kisslinger and R. A. Sorensen, Rev. Mod. Phys. 35, 853 (1963).
[21] A. E. L. Dieperink, H. P. Leenhouts, and P. J. Brussaard, Nucl. Phys. A116, 556 (1968).
[22] E. R. Flynn and P. D. Kunz, Phys. Lett. 68B, 40 (1977).
[23] C. K. Ross and R. K. Bhaduri, Nucl. Phys. A196, 369 (1972).
[24] K. Heyde, M. Waroquier, and P. Van Isacker, Phys. Rev. C 22, 1267 (1980).
[25] S. M. Abecasis, O. Givitarese, and F. Krmpotic, Phys. Rev. C 9, 39 (1973).
[26] J. Van Maldeghem, Lic. thesis, State University of Gent, 1980 (unpublished).
[27] J. Bron, W. H. A. Hesselink, A. Von Poelgeest, J. J. A. Zalmstra, M. J. Uitzinger, H. Verheul, K. Heyde, M. Waroquier, H. Vincx, and P. Van Isacker, Nucl. Phys. A318, 335 (1979).
[28] A. Van Poelgeest, Ph.D. thesis, Vrije Universiteit, Amsterdam, 1979 (unpublished).
[29] W. H. A. Hesselink (private communication).
[30] A. Van Poelgeest, J. Bron, W. H. A. Hesselink, K. Allaart, J. J. A. Zalmstra, M. J. Uitzinger, and H. Verheul, Nucl. Phys. A346, 70 (1980).
[31] J. Kantele, R. Julin, M. Luontama, A. Passoja, T. Pockolainen, A. Bäcklin, and N. G. Jonson, Z. Phys. A 289, 157 (1979).
[32] A. Bäcklin, N. G. Jonsson, R. Julin, J. Kantele,

M. Luontama, A. Passoja, and T. Pockolainen, Nucl. Phys. A351, 490 (1981).
[33]R. Julin, Ph.D. thesis, University of Jyväskylä, 1979 (unpublished).
[34]N. G. Jonson, Ph.D. thesis, University of Uppsala, 1979 (unpublished).
[35]A. Bohr and B. Mottelson, *Nuclear Structure* (Benjamin, New York, 1969), Vol. I, p. 379.
[36]V. Paar, in *Proceedings of the Fifteenth International Summer Meeting on Nuclear Physics and Nuclear Structure*, edited by A. H. Kukoč (Institute "B. Kidrič," Belgrade, 1972), p. 234.
[37]A. Bohr and B. Mottelson, *Nuclear Structure* (Benjamin, New York, 1975), Vol. II, pp. 174, 358, 552.
[38]A. S. Reiner, Nucl. Phys. 27, 115 (1961).
[39]Here, we use the relations $5\hbar\omega_2/(2C_2) = \beta_2^2 = B(E2; 0_1^+ \rightarrow 2_1^+)/[3/(4\pi)ZeR_0^2]^2$.
[40]B. F. Bayman and A. Lande, Nucl. Phys. 77, 1 (1966).
[41]J. Sau, K. Heyde, and M. Waroquier, Nucl. Phys. A298, 93 (1978).